




Article

Influence of Composition and Technological Factors on Variotropic Efficiency and Constructive Quality Coefficients of Lightweight Vibro-Centrifuged Concrete with Alkalized Mixing Water

Sergey A. Stel'makh ¹, Evgenii M. Shcherban' ¹, Alexey N. Beskopylny ^{2,*}, Levon R. Mailyan ³,
Besarion Meskhi ⁴, Denis Butko ⁵ and Alla S. Smolyanichenko ⁵

¹ Department of Engineering Geology, Bases, and Foundations, Don State Technical University, 344000 Rostov-on-Don, Russia; sergej.stelmax@mail.ru (S.A.S.); au-geen@mail.ru (E.M.S.)

² Department of Transport Systems, Faculty of Roads and Transport Systems, Don State Technical University, 344000 Rostov-on-Don, Russia

³ Department of Roads, Don State Technical University, 344000 Rostov-on-Don, Russia; lrm@aaanet.ru

⁴ Department of Life Safety and Environmental Protection, Faculty of Life Safety and Environmental Engineering, Don State Technical University, 344000 Rostov-on-Don, Russia; reception@donstu.ru

⁵ Department of Water Supply and Sewerage, Don State Technical University, 344000 Rostov-on-Don, Russia; den_111@mail.ru (D.B.); arpis-2006@mail.ru (A.S.S.)

* Correspondence: besk-an@yandex.ru; Tel.: +7-8632-738-454



Citation: Stel'makh, S.A.; Shcherban', E.M.; Beskopylny, A.N.; Mailyan, L.R.; Meskhi, B.; Butko, D.; Smolyanichenko, A.S. Influence of Composition and Technological Factors on Variotropic Efficiency and Constructive Quality Coefficients of Lightweight Vibro-Centrifuged Concrete with Alkalized Mixing Water. *Appl. Sci.* **2021**, *11*, 9293. <https://doi.org/10.3390/app11199293>

Academic Editors: Dario De Domenico and Kang Su Kim

Received: 15 August 2021

Accepted: 1 October 2021

Published: 6 October 2021

Publisher's Note: MDPI stays neutral with regard to jurisdictional claims in published maps and institutional affiliations.



Copyright: © 2021 by the authors. Licensee MDPI, Basel, Switzerland. This article is an open access article distributed under the terms and conditions of the Creative Commons Attribution (CC BY) license (<https://creativecommons.org/licenses/by/4.0/>).

Abstract: Alkalinization technology and its application to obtain high-performance concrete compositions is an urgent scientific problem that opens opportunities for improving building structures. The article is devoted to the new technology of manufacturing reinforced concrete structures with low energy consumption, resource, and labor intensity based on the improved variotropic configuration of vibro-centrifuged concrete using activated water with high pH. The synergistic effect of the joint use of the proposed novel solutions has been theoretically and experimentally proved. Thus, growth in physical and mechanical characteristics of up to 15–20% was obtained, the structure and its operational ability were improved (the effectiveness of structural improvement, expressed as a percentage, reached values over 70%, concerning control samples). A positive effect on the properties of vibro-centrifuged concrete over the entire thickness of the annular section has been revealed. A method for controlling the integral characteristics of concrete has been obtained. The possibility of regulating the variotropic structure and controlling the differential characteristics of vibro-centrifuged concrete has been established. An assessment of the constructive quality and variotropic efficiency of vibro-centrifuged concrete was carried out, and new calculated dependencies were proposed, expressed in the form of relative coefficients.

Keywords: fiber-reinforced concrete; alkali-activated concrete; vibro-centrifuged concrete; variotropic structure; mechanical strength; high-performance concrete; coefficient of constructive quality

1. Introduction

In recent years, various kinds of activations have drawn significant attention from researchers to improve the technology of high-performance concrete and obtain effective building products and structures [1–6]. However, it is known that the concept of activation often goes hand in hand with the idea of high energy and high resource intensity [7]. The decrease in these indicators is an important scientific problem. Therefore, an outstanding and urgent direction is the search for technology for activating building materials, products, and structures, mainly made of reinforced concrete, with low energy, resource, and labor intensity. At the same time, the goal of activation must be achieved, namely, high physical, mechanical, and structural characteristics of the manufactured concrete products and

structures made of them, their low weight and versatility, expressed in the possibility of using such products, constructions, and materials in complex conditions.

In this regard, activation is seen as a perspective direction, using not physical—associated with influences of various kinds, expending magnetic, electrical, thermal, and other energy—but chemical activation. As a result of activation, an effect on the formation of the improved structure is obtained and the new properties of the concrete are developed at the stage of the interaction of the participating components. Therefore, it seems promising to use water alkalization technology and its subsequent use as mixing water for activated concrete. At the same time, previously, it was established [8] that the technology of vibro-centrifugation for obtaining reinforced concrete structures of a variotropic form is the most rational and effective.

It is known [9] that the process of forming a variotropic structure lies in the fact that the mold rotates at low speed and the material is uniformly distributed over the annular section. Then, with an increase in the rotation speed, under the influence of centrifugal pressure, part of the mixing water is squeezed out of the cement paste together with highly dispersed fractions. As a result, there is a convergence of larger aggregate particles, which achieves the highest degree of compaction of the concrete mixture of the outer layer. The values of the compressing and hydrostatic pressure vary unevenly along with the wall thickness of the product. At the outer wall of the product surface, the compressing and hydrostatic pressure reach maximum values, while at the inner wall, as a rule, they are minimal. Due to the pressure difference, the liquid phase is squeezed out of the entire wall thickness of the product unevenly. As a result, most of the liquid is pressed out of the outer concrete layers. Almost no liquid separates from the inner layer, which is explained by the very low compressing pressure, the value of which is practically zero.

The mechanical and physical properties of alkali-activated cement (AAC) concrete with a mixed binder were studied in [10]. Various starting materials were investigated such as fly ash (FA), ground granular blast furnace slag (GGBS), silica fume (SF), and metakaolin (MK). The study results showed that the properties of AAC are highly dependent on the combinations and type of raw materials used [10–13].

In [14], the characteristics of prefilled concrete prepared using an alkali-activated cement slurry as an adhesive binder were evaluated. In addition, various combinations of slag and fly ash without fine aggregate as filler were considered and different solution-to-solid ratios. The results showed that the alkali-activated slurry had a better flow and compressive strength characteristics than conventional slurry. As a result, the mechanical properties of the pre-laid aggregate concrete have been significantly improved [14–17].

Works [18,19] are devoted to the properties of light ash-slag concrete, activated with alkali. The effect of different water/solid (W/S) ratios on the properties of normal weight concrete/light fly ash and alkali-activated slag were studied. The relative performance of mixtures of AAC with limestone and lightweight fly ash aggregates as coarse aggregates was also compared with conventional concrete with ordinary Portland cement (OPC) in terms of strength, deformability, and fracture behavior. The results showed that AAC has higher tensile strength, brittleness, and lower modulus than its cement-based counterpart. As the W/S ratio decreases, the density, strength, and elastic modulus of AAC increase. However, the influence of the W/S ratio on the mechanical properties of LAAC with lightweight porous aggregates was less than that of heavy AAC [18,19].

Physical properties of alkali-activated materials (AAMs) were investigated in [20–23]. It has been found that the alkali content is often considered the main characteristic of alkali-activated materials. However, the SiO₂ content can also play an important role. The results of these works show that the strengths of AAMs are highly dependent on the type of hardening. For example, curing in an aqueous medium reduced the strength of the samples compared to the models covered with foil. Furthermore, physical properties depend on the curing method and the activator's composition; some concretes with high strength showed very low frost resistance [20–23].

Mechanical properties and durability of alkali-activated carbon slag concrete were carried out in [24–27]. In this case, the new geopolymer is recognized as a potential alternative cementitious material to OPC, which is used to reduce carbon emissions and efficiently treat waste. Therefore, work [21] mainly studies alkali-activated carbon-slag concrete (ACSC) prepared using coal and a complex activator Na_2SiO_3 and NaOH . The results show that ACSC showed high compressive strength at an early age, and the degree of compactness and structure uniformity was better compared to OPC when the coal rock replacement ratio was less than 50% [24–27].

In [28], the effect of water content on the mechanical strength and microstructure of alkali-activated FA/ground granulated blast furnace slag (GGBFS), solidifying in cold and polar regions, was investigated. The effect of water content on the properties of an alkali-activated binder solution cured at $-5\text{ }^\circ\text{C}$ was investigated. FA and GGBFS were used as binders. The results showed that lower water content is beneficial for improving the early strength of the mortar at a curing temperature of $-5\text{ }^\circ\text{C}$, while it has little effect on long-term strength. These results are relevant for the design and construction of geopolymer concretes in cold regions [28].

Characteristics of concrete, reinforced with steel fibers, activated with alkali, slag, and FA, containing secondary aggregates from recycled concrete and sand are given in [29]. This study evaluated the performance of alkali-activated slag and FA concrete made from recycled concrete aggregates (RCA) and reinforced with steel fibers [29].

In [30], the strength of a building material containing an alkali-activated lightweight aggregate based on fly ash, was calculated. In addition, this study examined the durability of a mortar consisting of LWA activated alkaline ash and LWA expanded clay (EC). The mortar used by FA 6M LWA has comparable water absorption capillary resistance of the chlorides to the EC LWA reference mortar [30].

The work [31] presents the ultrasonic strength of cement mixtures activated with alkalis. In this study, the change in setting time and strength of AAC blends was studied using the ultrasonic method. The effect of binder content, ratio of alkaline solid to binder (AS/B), ratio of sodium silicate to solid sodium hydroxide (SS/SH), and ratio of total water to total solid binder (TW/TS) on strength and setting time are also considered [31].

All these works are devoted to simple structures of concrete, yet are associated with reasonably resource-intensive technologies. We propose and describe below a low-resource-intensive method for controlling the variatropic properties and structure formation of variatropic concretes due to the chemical activation of mixing water.

In previous studies by the team of authors [8,9], the positive influence of the rational variatropic structure formed in concrete by controlling the technological process on the final performance characteristics of concrete and products and structures made of them was studied and established. However, the possibility of regulating the structure and controlling properties using the chemical activation of water was not previously considered, i.e., a low-resource-intensive method, which at the same time gives a great effect in terms of a qualitative increase in characteristics.

Thus, the aim of our study was to assess the influence of composition and technological factors on variatropic efficiency and constructive quality coefficients of lightweight vibro-centrifuged concrete with alkalized mixing water.

The novelty of this study lies in the theoretical substantiation and experimental confirmation that the use of activated water in the manufacture of lightweight vibro-centrifuged concretes leads to an improvement in both absolute strength characteristics and relative coefficients. Additionally, vibro-centrifugation technology makes it possible to obtain a perfect variatropic structure. This is justified by the fact that water with a higher pH value contributes to an increase in the degree of hydration of the cement and the improvement of the directional structure formation of concrete.

In this regard, a working hypothesis has been developed: it is possible to obtain an improved variatropic structure of vibro-centrifuged concrete by using mixing water with a high pH, obtained as a result of alkaline action. Thus, a synergistic effect will be achieved

and gains in physical and mechanical characteristics will be obtained, the structure will be improved, and thereby the operational ability of such products and structures will be improved.

2. Materials and Methods

2.1. Materials

During the research, no additive Portland cement of the PC 500 D0 brand was used, the physical and mechanical characteristics of which are presented in Table 1. Table 2 shows the chemical and mineralogical composition of Portland cement.

Table 1. Physical and mechanical characteristics of Portland cement PC 500 D0.

Indicator Title	Value
Compressive strength at the age of 28 days, MPa	55.7
Time of concrete hardening, min	
-Start	165
-Finish	270
Fineness of grinding, passing through a sieve No. 008, %	97.8
Specific surface, m ² /kg	380
Normal consistency of cement paste, %	25.5

Table 2. Mineralogical and chemical composition of Portland cement.

Cement Grade	Mineralogical and Chemical Composition, %										
	C ₃ S	C ₂ S	C ₃ A	C ₄ AF	MgO	SO ₃	Al ₂ O ₃	Fe ₂ O ₃	Na ₂ O + K ₂ O	CaO	SiO ₂
PC 500 D0	63.5	16.0	6.5	14.0	0.94	0.76	5.3	4.58	0.62	66.2	21.6

Granite crushed stone of Pavlovsk Nerud OJSC (Pavlovsk, Voronezh region, Russia) with a fraction of 5–20 mm was used as a large dense aggregate and expanded clay gravel as porous. The physical and mechanical characteristics of a large dense and porous aggregate are presented in Tables 3 and 4.

Table 3. Physical and mechanical characteristics of crushed stone.

Fraction	Bulk Density, kg/m ³	True Density, kg/m ³	Crushing, wt %	Lamellar Grain Content and Needle-Shaped Forms, wt. %	Void Ratio, %
5–20	1430	2660	11.4	9.5	47

Table 4. Physical and mechanical characteristics of expanded clay gravel.

Fraction	Bulk Density, kg/m ³	True Density, kg/m ³	Strength by GOST 32496–2013, MPa	Void Ratio, %
5–20	480	880	2.1	46

Quartz sand was used as a dense fine aggregate, the physical characteristics of which are presented in Table 5.

Table 5. Physical characteristics of dense fine aggregate.

Grain Composition							Passing	Fineness Modulus	Content of Dust and Clay Particles, %	True Density, kg/m ³	Bulk Density, kg/m ³
Sieve Size, mm											
Retained	Retained and Cumulative Retained, %										
Through a Sieve No 0.16, wt. %											
10	5	2.5	1.25	0.63	0.315	0.16					
0	0	0.17	1.39	8.86	45.80	41.03	2.49	1.66	1.1	2610	1438
		0.17	1.56	10.42	56.21	97.25	99.74				

2.2. Methods

In the study, water activated with alkali and purified by a sorbent with different pH levels of an aqueous solution was used. Water activation was carried out by purification, which was filtered through sorbent-activated biochar from agricultural waste—rice straw. The technology for obtaining activated water was followed in strict accordance with the methodology [32].

For the manufacture of vibro-centrifuged samples, an experimental laboratory vibro-centrifuge was used. A schematic diagram of this installation and a detailed description are presented in [33]. Additionally, in [34,35], the mode of forming prototypes of vibro-centrifuged concretes is described.

The study used:

- technological equipment—laboratory concrete mixer BL-10 (OOO “ZZBO”, Russia, Chelyabinsk region, Zlatoust); laboratory vibrating platform SMZh-539-220A (OOO “IMASH”, Armavir, Russia);
- testing equipment—hydraulic press IP-1000 (OOO NPK TEKHMASH, Neftekamsk, Republic of Bashkortostan, Russia), tensile testing machine R-50 (OOO IMash, Armavir, Russia);
- measuring instruments—stationary pH meter Starter 2100 (OHAUS CIS, Russia) measuring metal ruler 500 mm; laboratory scales; device for measuring deviations from the plane NPL-1; device for measuring deviations from perpendicularity NPR-1.

The technological sequence of concrete mix molding was as follows.

The original components are dosed and mixed in a concrete mixer. Then, reaching the required workability of the mixture with a cone draft of 1–4 cm, the mixture is placed in a particular mold located on a vibro-centrifuge. Finally, the drive is turned on and vibro-centrifugation is performed until the planned samples of the annular cross-section are obtained (according to the modes specified in [33]) for their further processing.

In total, four basic samples of annular cross-section were manufactured and tested with the following dimensions:

outer diameter $D = 450$ mm;
 inner diameter of the hole $d = 150$ mm;
 total height $H = 1200$ mm.

The technique of making prototypes for determining the strength integral and differential characteristics of concrete is described [8]. The experimental research program is shown in Figure 1.

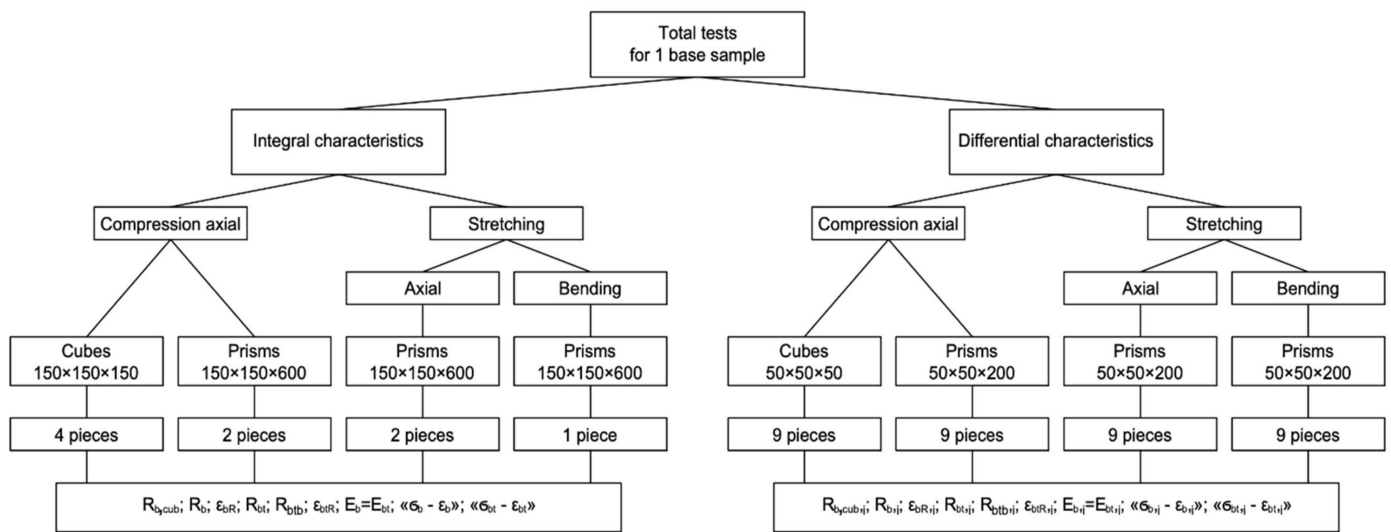


Figure 1. Program of experimental research (sizes in mm).

Measurements of the concrete strains of the test prisms were carried out by a chain of strain gauges with a side length of 50 mm and dial indicators with a graduation value of 0.001 mm. The strain measurement of a prism sample under axial compression is shown in Figure 2a,b.

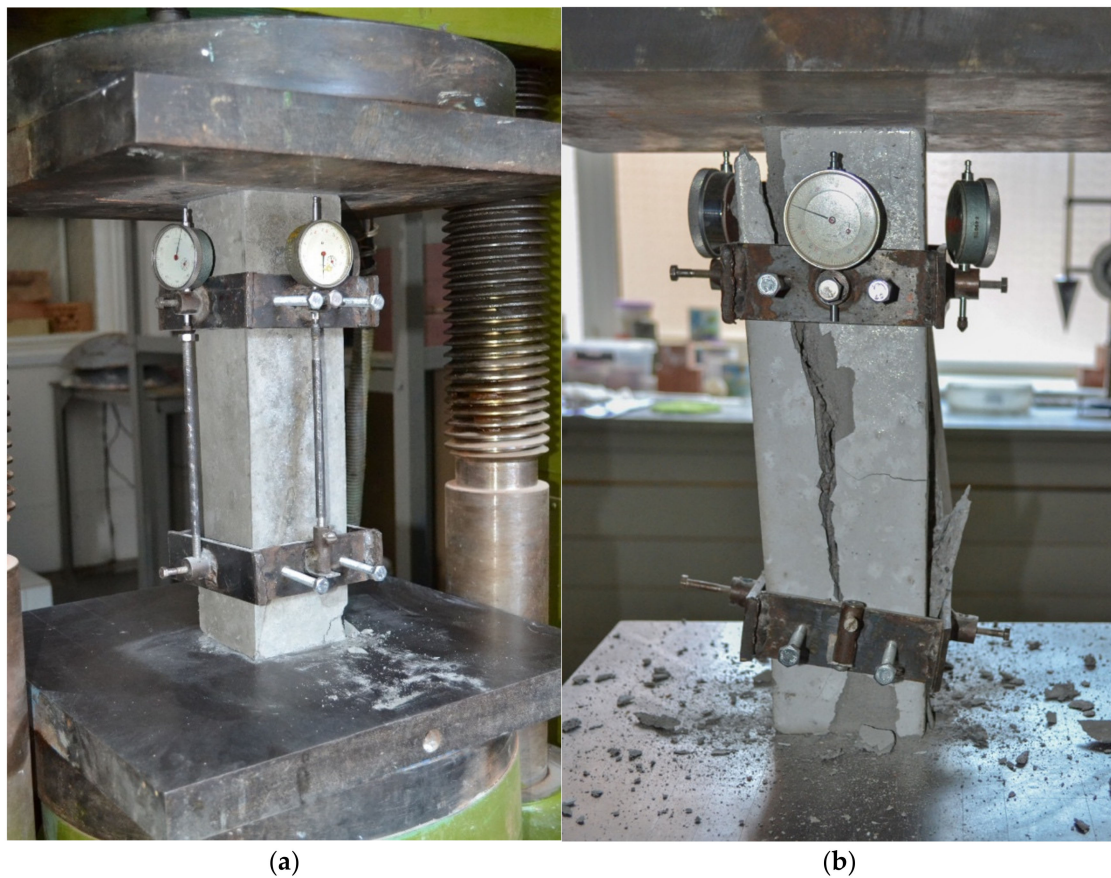


Figure 2. Photo of strain measurement of the prism sample under axial compression (a); sample after collapse (b).

Compression, axial tensile, and flexural tensile tests were carried out in accordance with the requirements of GOST 10180 “Concretes. Methods for strength determination using reference specimens” [36]. Axial compression tests were carried out in accordance

with the requirements of GOST 24452 “Concretes. Methods of prismatic, compressive strength, modulus of elasticity, and Poisson’s ratio determination” [37].

The values of the coefficients of strength and deformative variatropic efficiency were calculated using the following formulas:

$$K_{R_{b,cub}} = \frac{\overline{R_{b,cub}} - R_{b,cub}}{R_{b,cub}} \times 100, \% \quad (1)$$

where $R_{b,cub}$ is cubic compressive strength, MPa;

$\overline{R_{b,cub}} = \frac{\sum R_{b,cub,i}}{n}$ is the average value when calculating differential characteristics, MPa; i is layer number; n is the number of layers.

$$K_{R_b} = \frac{\overline{R_b} - R_b}{R_b} \times 100, \% \quad (2)$$

where R_b is the prismatic compressive strength, MPa;

$\overline{R_b} = \frac{\sum R_{b,i}}{n}$ is the average value when calculating differential characteristics, MPa.

$$K_{R_{btb}} = \frac{\overline{R_{btb}} - R_{btb}}{R_{btb}} \times 100, \% \quad (3)$$

where R_{btb} is the tensile strength in bending, MPa;

$\overline{R_{btb}} = \frac{\sum R_{btb,i}}{n}$ is the average value when calculating differential characteristics, MPa.

$$K_{R_{bt}} = \frac{\overline{R_{bt}} - R_{bt}}{R_{bt}} \times 100, \% \quad (4)$$

where R_{bt} is the axial tensile strength, MPa;

$\overline{R_{bt}} = \frac{\sum R_{bt,i}}{n}$ is the average value when calculating differential characteristics, MPa.

$$K_{\varepsilon_{bR}} = \frac{|\overline{\varepsilon_{bR}} - \varepsilon_{bR}|}{\varepsilon_{bR}} \times 100, \% \quad (5)$$

where ε_{bR} is ultimate strain during axial compression, $\text{mm/m} \times 10^{-3}$;

$\overline{\varepsilon_{bR}} = \frac{\sum \varepsilon_{bR,i}}{n}$ is the average value when calculating differential characteristics, MPa.

$$K_{\varepsilon_{btR}} = \frac{|\overline{\varepsilon_{btR}} - \varepsilon_{btR}|}{\varepsilon_{btR}} \times 100, \% \quad (6)$$

where ε_{btR} is ultimate strain during axial tension, $\text{mm/m} \times 10^{-4}$;

$\overline{\varepsilon_{btR}} = \frac{\sum \varepsilon_{btR,i}}{n}$ is the average value when calculating differential characteristics, MPa

$$K_{E_b=E_{bt}} = \frac{\overline{E_b = E_{bt}} - E_b = E_{bt}}{E_b = E_{bt}} \times 100, \% \quad (7)$$

where $E_b = E_{bt}$ is the integral modulus of elasticity, GPa;

$\overline{E_b = E_{bt}} = \frac{\sum E_{b,i} = E_{bt,i}}{n}$ is the average value when calculating differential characteristics, GPa.

The coefficients of constructive quality (CCQ) for different types of strength were calculated using the following formulas:

$$CCQ_{R_{b,cub}} = \frac{R_{b,cub}}{\rho} \quad (8)$$

where $R_{b,cub}$ is cubic compressive strength, MPa.

ρ is the density of concrete, g/cm³.

$$CCQ_{R_b} = \frac{R_b}{\rho} \quad (9)$$

where R_b is prismatic compressive strength, MPa.

$$CCQ_{R_{btb}} = \frac{R_{btb}}{\rho} \quad (10)$$

where R_{btb} is the tensile strength in bending, MPa.

$$CCQ_{R_{bt}} = \frac{R_{bt}}{\rho} \quad (11)$$

where R_{bt} is the axial tensile strength, MPa.

For the manufacture of vibro-centrifuged samples of annular cross-section, heavy concrete of class B30 with the required workability grade corresponding to the draft of the cone of 1–4 cm (method according to [38]) was designed in accordance with previously developed recommendations [33–35]. The content of coarse aggregate fractions is represented by the following ratio: 60%—fraction 10–20 mm; 40%—fraction 5–10 mm. The parameters of the composition of the concrete mixture obtained as a result of calculations are reflected in Table 6.

Table 6. Parameters of the composition of the concrete mixture.

Indicator	W/C	Absolute Volume of Cement Paste, l	Absolute Volume of Aggregates, l, at a Ratio $r = S/CS = 0.4$	Weight of Cement in the mix, kg/m ³	Weight of Crash Stone in the Mix, kg/m ³	Weight of Sand in the Mix, kg/m ³
Indicator value	0.38	319	1805	400	1290	515

During the lightweight vibro-centrifuged concrete manufacture, part of the volume of dense aggregate was replaced with the same volume of porous in an amount of 30%. Cement consumption and S/CS (Sand/Crash stone) ratio remained unchanged.

In accordance with the requirements of GOST 23732–2011 “Water for concrete and mortars. Specifications” [39], the pH value of water should be not less than 4 and not more than 12.5. The pH was determined by a potentiometric method using a stationary Starter 2100 pH meter (OHAUS SNG, Russia) with glass electrodes with a pH range from 0 to 14 and a measurement error not exceeding ± 0.1 . To determine the pH, water was taken from 10 to 50 mL into a glass beaker with a capacity of 50 to 100 mL. The pH was determined according to the instructions for the device.

The section was divided into three layers, outer, middle, and inner, and samples were cut from each layer—cubes or prisms, depending on the type of test. Sawing of the samples was carried out on a stone cutting machine; samples testing was carried out using a hydraulic press [8].

3. Results

The results of experimental studies of the influence of the pH level of activated water on the coefficients of strength and deformative variatropic efficiency and the coefficients of constructive quality of lightweight vibro-centrifuged concrete are presented in Figures 3–5. The results obtained on the basis of testing of prototypes of vibro-centrifuged concrete made using activated water are presented in Tables 7 and 8.

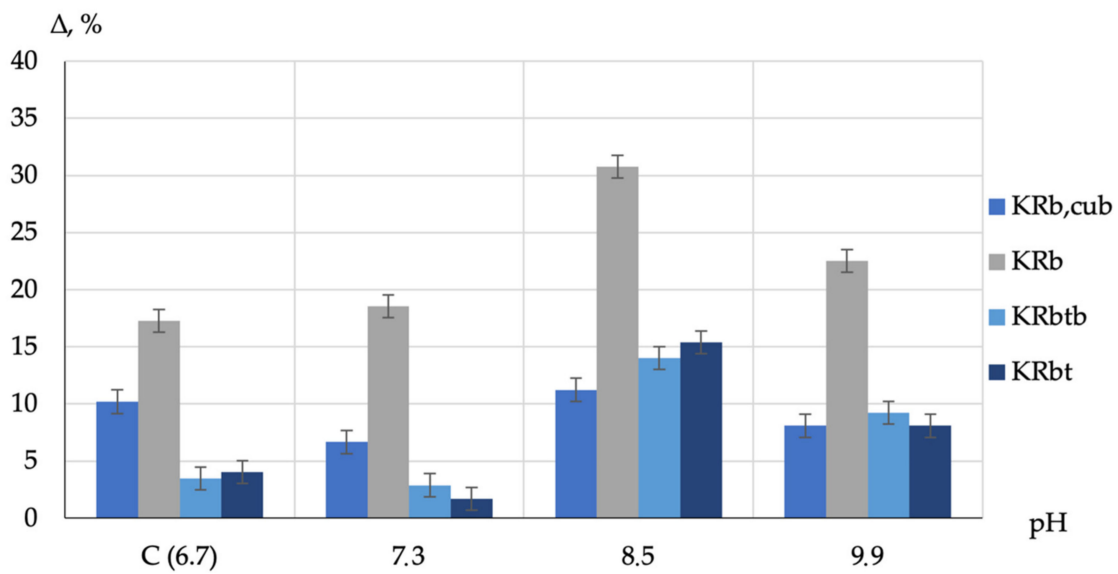


Figure 3. Dependence of the change in the coefficients of the strength variatropic efficiency of vibro-centrifuged concretes on the pH level of activated water (C is the control composition; Δ is the value of the change in the coefficients of the strength variatropic efficiency).

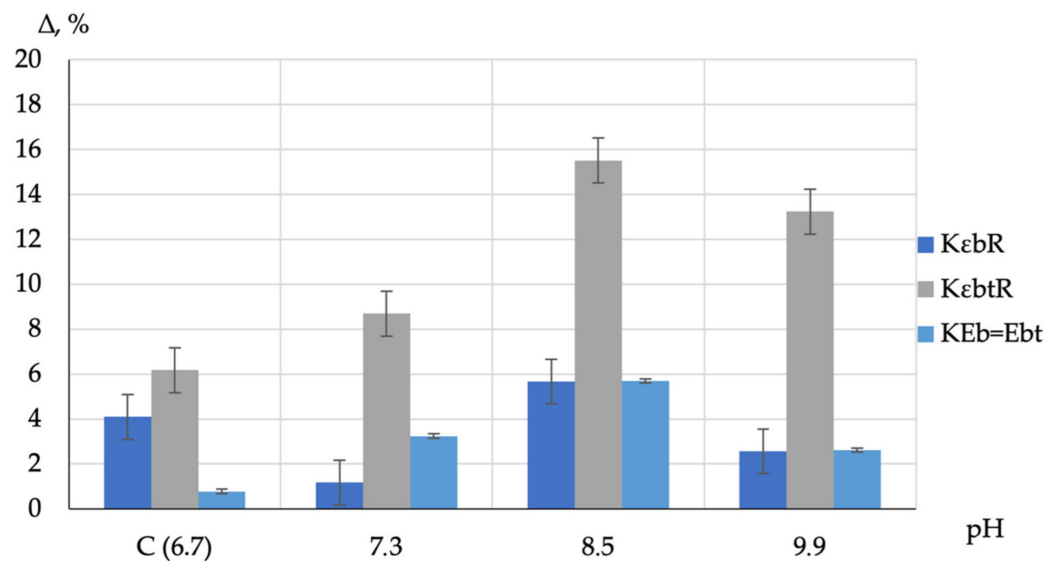


Figure 4. Dependence of the change in the coefficients of the strain variatropic efficiency of vibro-centrifuged concretes on the pH level of activated water (see Figure 3; C is the control composition; Δ is the value of the change in the coefficients of the strength variatropic efficiency).

These tables show the average values of the strength and strain characteristics of concrete. So, for the integral cube strength, the average value was calculated from the test results of four cube specimens included in the series, and the average value of the integral prismatic strength and axial tensile strength was determined from the test results of two sample prisms included in the series. The values of the integral strength characteristics of individual samples in the series differed by no more than 8% from the average values. As for the differential strength and deformation characteristics, the average values for the cube strength were calculated from the test results of three sample cubes, and for the prismatic strength, axial tensile strength, and bending tensile strength, according to the test results of three prism samples. The deviations of the values of the strength differential characteristics of individual samples in the series differed by no more than 9% from the average values.

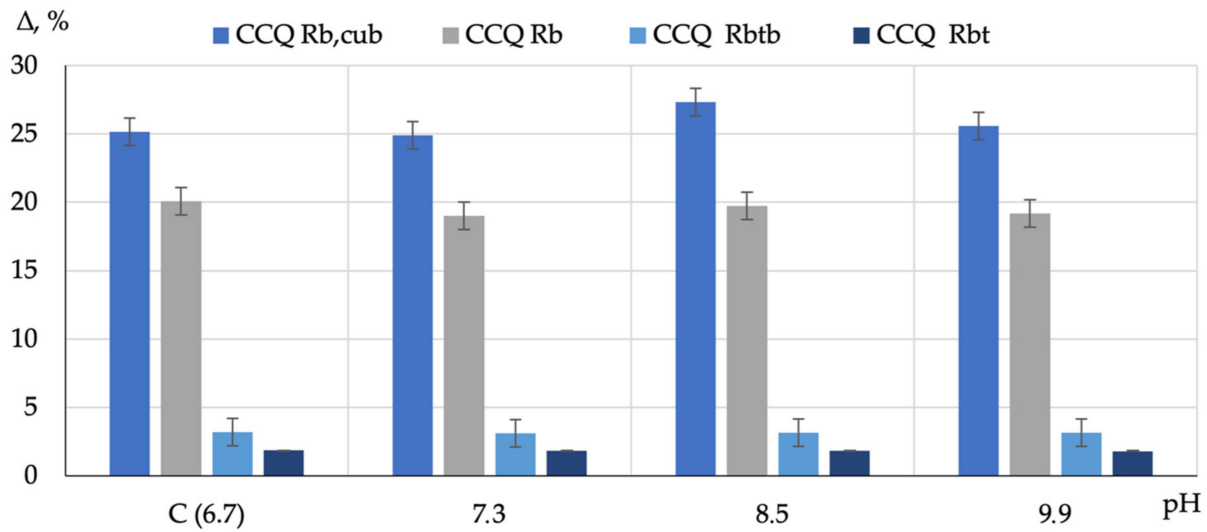


Figure 5. Dependence of the change in the structural quality coefficients of vibro-centrifuged concretes on the pH level of activated water (see Figure 3; C is the control composition; Δ is the value of the change in the coefficients of the strength variatropic efficiency).

Table 7. Integral strength and strain characteristics of prototypes of vibro-centrifuged concrete.

Concrete Characteristic	Control Composition (Heavy Concrete on Non-Activated Water, pH = 6.7)	Lightweight Concrete		
		pH = 7.3	pH = 8.5	pH = 9.9
$\rho, \text{ kg/m}^3$	2398	2073	2069	2042
$R_{b, \text{ cub}}, \text{ MPa}$	61.8	50.8	55.7	52.8
$R_b, \text{ MPa}$	49.4	38.9	40.3	39.6
$R_{btb}, \text{ MPa}$	7.9	6.3	6.4	6.5
$R_{bt}, \text{ MPa}$	4.6	3.7	3.8	3.7
$\epsilon_{bR}, \text{ mm/m} \times 10^{-3}$	1.79	2.28	2.41	2.34
$\epsilon_{btR}, \text{ mm/m} \times 10^{-4}$	1.18	1.38	1.44	1.46
$E_b = E_{bt}, \text{ GPa}$	38.7	34.2	36.3	35.7

Table 8. Differential strength and deformation characteristics of prototypes of vibro-centrifuged concrete.

Concrete Characteristic	Control Composition (Heavy Concrete on Non-Activated Water, pH = 6.7)			Lightweight Concrete								
				pH = 7.3			pH = 8.5			pH = 9.9		
	VC ₁	VC ₂	VC ₃	VC ₁	VC ₂	VC ₃	VC ₁	VC ₂	VC ₃	VC ₁	VC ₂	VC ₃
$R_{b, \text{ cub}}, \text{ MPa}$	38.2	74.0	92.1	38.1	53.3	71.1	38.0	69.9	78.0	38.3	60.7	72.2
$R_b, \text{ MPa}$	32.5	62.9	78.3	32.4	45.3	60.5	32.3	59.4	66.3	32.6	51.6	61.4
$R_{btb}, \text{ MPa}$	4.6	8.9	11.1	4.6	6.4	8.5	4.3	8.4	9.4	4.6	7.3	9.4
$R_{bt}, \text{ MPa}$	2.7	5.3	6.4	2.7	3.7	5.0	2.7	4.9	5.5	2.7	4.3	5.1
$\epsilon_{bR}, \text{ mm/m} \times 10^{-3}$	2.11	1.66	1.38	2.23	2.45	2.08	2.26	2.59	1.97	2.25	2.58	2.01
$\epsilon_{btR}, \text{ mm/m} \times 10^{-4}$	1.31	1.11	0.91	1.30	1.27	1.21	1.20	1.24	1.21	1.3	1.31	1.19
$E_b = E_{bt}, \text{ GPa}$	28.2	41.8	47.0	28.2	37.6	40.1	28.1	41.7	45.3	28.0	39.8	42.1

VC₁—the inner layer; VC₂—middle layer; VC₃—outer layer.

The minimum and maximum values of the characteristics in diagrams of Figures 3–7 are determined based on the statistical error on the assumption that the random variable has a normal distribution, and the confidence limit is taken at the level of 80%.

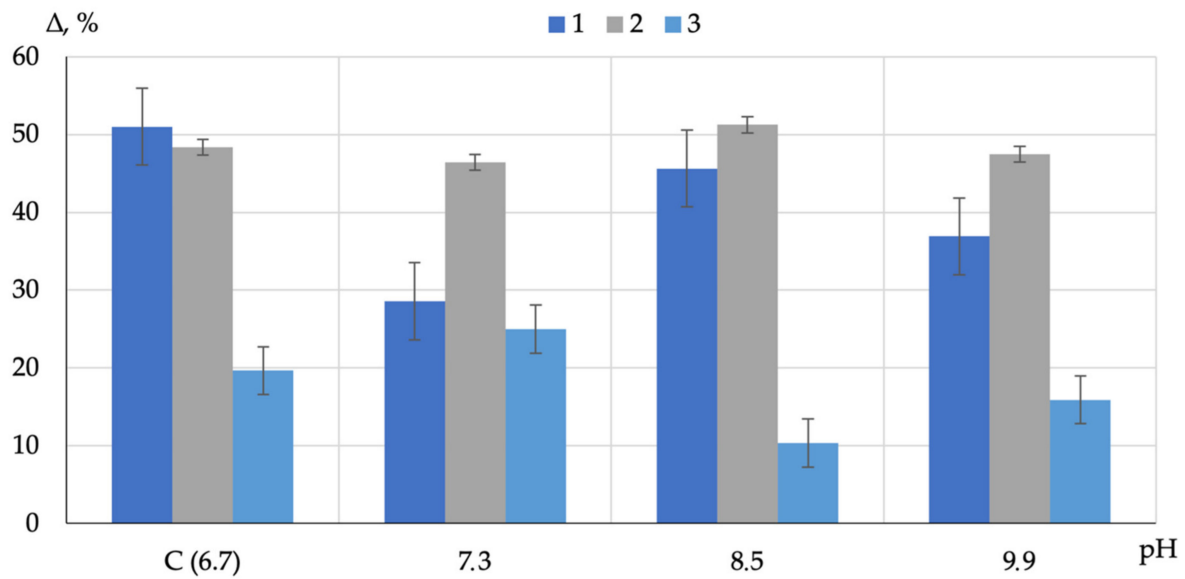


Figure 6. Dependence of the difference between the strength characteristics of layers of variatropic sections of vibro-centrifuged concrete on the pH level of activated water (1—the difference between the inner and middle layer; 2—the difference between the inner and outer; 3—the difference between the middle and outer; C is the control composition; Δ is the value of the change in the coefficients of the strength variatropic efficiency).

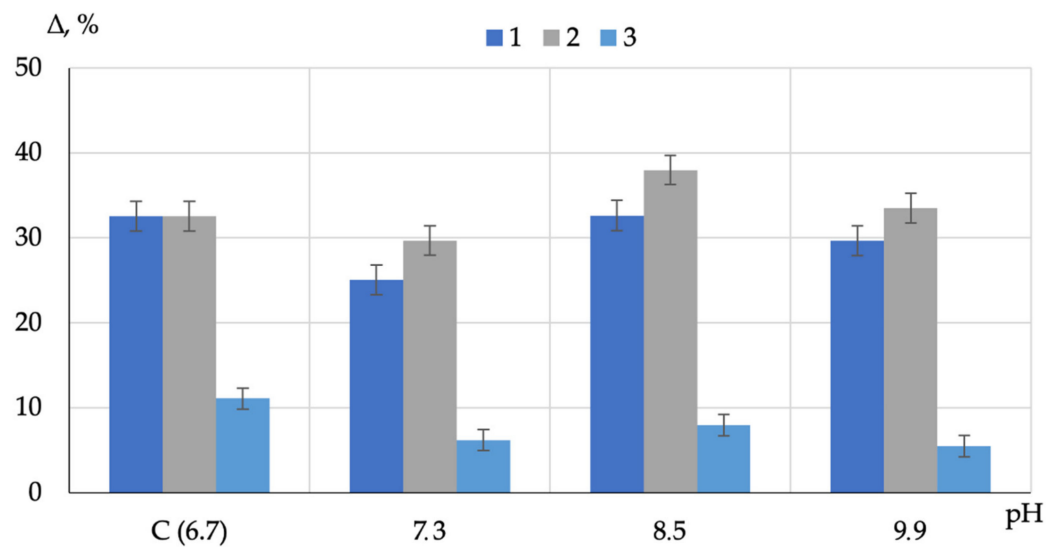


Figure 7. Dependence of the difference between the elastic moduli of different layers of variatropic sections of vibro-centrifuged concrete on the pH level of activated water (C is the control composition; Δ is the value of the change in the coefficients of the strength variatropic efficiency).

Table 7 shows that in lightweight vibro-centrifuged concrete made on activated water, with an increase in the pH level from 7.3 to 8.5, an increase in strength is observed. This fact is due to an increase in the degree of cement hydration and an increase in the homogeneity of the concrete structure. When the pH level rises from 8.5 to 9.9, the strength characteristics of concrete decrease. The maximum changes in strength and deformation characteristics were recorded at pH = 8.5.

Differential strength and strain characteristics of prototypes of vibro-centrifuged concrete are shown in Table 8.

After analyzing the obtained graphical dependences of changes in the coefficients of strength and deformative variatropic efficiency, it was found that the values of these coefficients in lightweight vibro-centrifuged concretes are an order of magnitude higher in comparison with heavy vibro-centrifuged concrete. Additionally, with an increase in

the pH of activated water, there is a clear tendency to increase the coefficients of strength and deformation efficiency in lightweight vibro-centrifuged concretes, and their maximum values were recorded when using activated water with a pH of 8.5.

As for the coefficients of constructive quality, it can be seen from Figure 5 that the values of these coefficients for both heavy and lightweight vibro-centrifuged concrete differ insignificantly. A slight increase in the values of the coefficients of constructive quality was recorded for lightweight vibro-centrifuged concretes made on activated water with a pH = 8.5.

It is known from the normative and technical documents [39] that the maximum permissible pH value for water for concrete is 12.5.

After analyzing the theoretical basis of the question, a hypothesis was put forward that the real efficiency of the mixing water used is limited by the pH value equal to 10, due to the further transformation of the medium into a highly alkaline one, and the achievement of values above 12.5 is completely unacceptable.

In this regard, when drawing up the program of experimental studies, we determined the assumed range of pH values, varying from 7 to 10. The midpoint was taken to be the assumed optimal pH equal to 8.5. During the practical leaching of water, the values of pH = 7.3, pH = 8.5, pH = 9.9 were obtained. A study has been carried out in this range. Based on the results of the experimental study, our hypothesis on the effectiveness of water with pH = 8.5 was confirmed. This value was recorded as rational and recommended for to prepare vibrated lightweight concrete with the best physical, mechanical, and structural characteristics.

Additionally, an assessment was made of the effect of the pH of activated water on the variatropy of lightweight vibro-centrifuged concretes, namely, the difference between the strength and deformation characteristics of different layers of variatropic sections (Δ) was determined as a percentage.

Thus, the difference between the strength characteristics of different layers of variatropic sections for lightweight vibro-centrifuged concrete made on activated water with a pH of 7.3 was:

- between the inner and middle layer—29%;
- between the inner and outer layers—46%;
- between the middle and outer layer—25%.

For lightweight vibro-centrifuged concrete made with activated water with pH = 8.5:

- between the inner and middle layer—46%;
- between the inner and outer layers—51%;
- between average and external—10%.

For lightweight vibro-centrifuged concrete made with activated water with pH = 9.9, this difference was:

- between the inner and middle layer—37%;
- between the inner and outer layers—47%;
- between the middle and outer layer—16%.

As for the difference between the moduli of elasticity of different layers of variatropic sections, then for lightweight vibro-centrifuged concrete made on activated water with a pH of 7.3, it was:

- between the inner and middle layer—25%;
- between the inner and outer layers—30%;
- between the middle and outer layer—6%.

For lightweight vibro-centrifuged concrete made with activated water with pH = 8.5:

- between the inner and middle layer—33%;
- between the inner and outer layers—38%;
- between the middle and outer layer—8%.

For lightweight vibro-centrifuged concrete made with activated water with pH = 9.9:

- between the inner and middle layer—30%;
- between the inner and outer layers—33%;
- between the middle and outer layer—5%.

Thus, it was found that with an increase in the pH level of activated water, variatropy also increases, which is expressed in an increase in the difference in characteristics between the inner and outer layers.

A graphic interpretation of the assessment of the difference between the strength characteristics and the modulus of elasticity of various layers of variatropic sections of lightweight and heavy vibro-centrifuged concretes is presented in Figures 6 and 7.

According to the test results, the compression diagrams “ $\epsilon_b-\sigma_b$ ” and tension “ $\epsilon_{bt}-\sigma_{bt}$ ” were plotted. Graphic dependences “stress—strain” are shown in Figures 8–11.

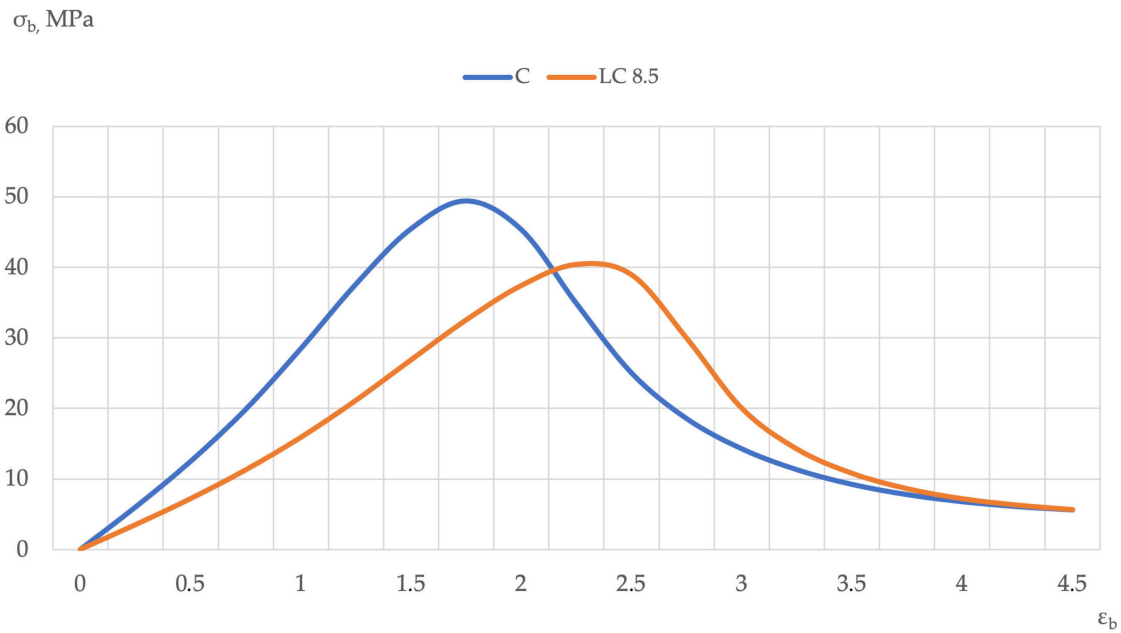


Figure 8. Diagram “stress—strain” in compression for the integral characteristics of vibro-centrifuged concrete (C—control composition: heavy concrete on non-activated water, LC 8.5—lightweight concrete on activated water with pH = 8.5).

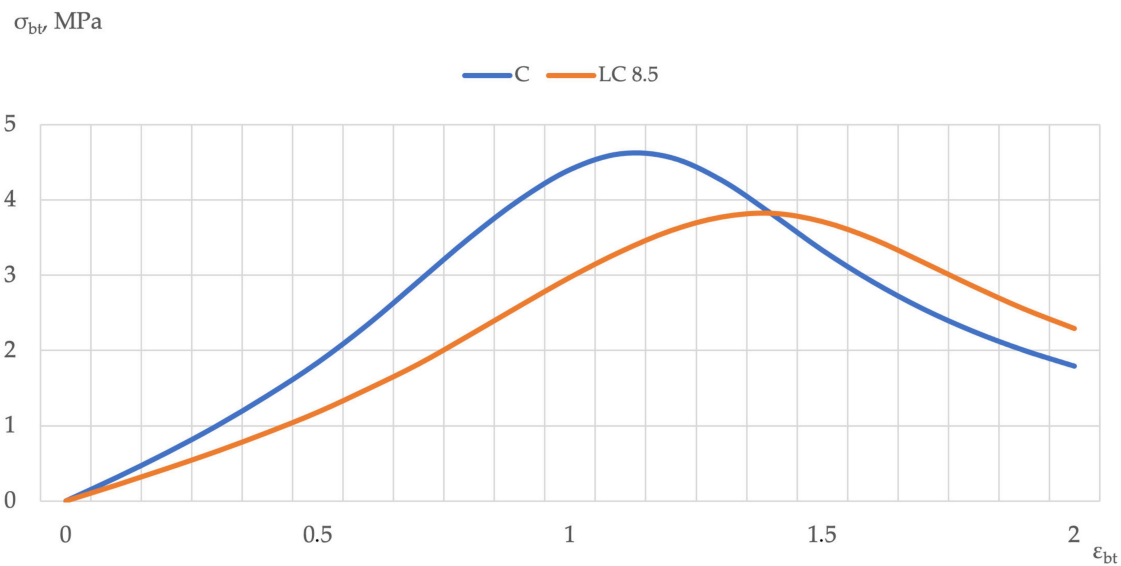


Figure 9. Diagram “stress—strain” in tension for the integral characteristics of vibro-centrifuged concrete (see Figure 8; C—control composition: heavy concrete on non-activated water, LC 8.5—lightweight concrete on activated water with pH = 8.5).

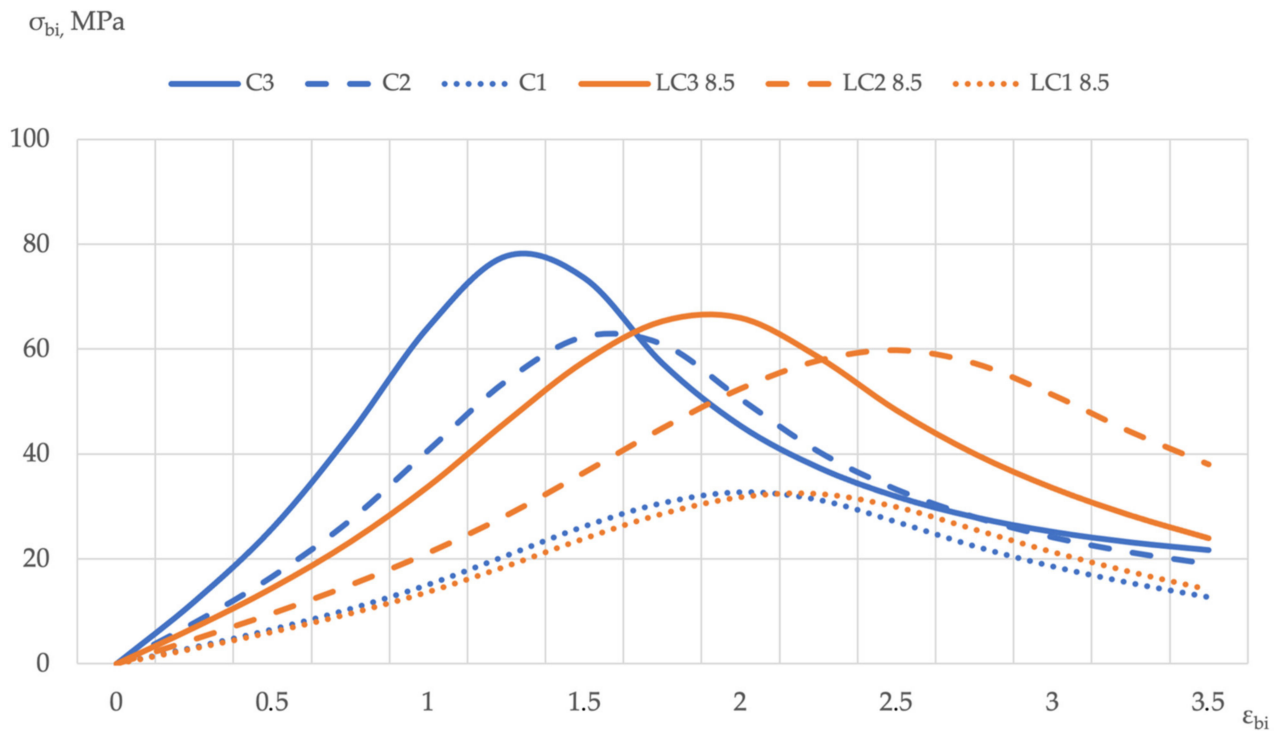


Figure 10. Diagram of “stress—strain” under compression for the differential characteristics of vibro-centrifuged concrete (C1, C2, C3—respectively the inner, middle, and outer layer of the control concrete composition; LC1 8.5, LC2 8.5, LC3 8.5—respectively the inner, middle, and outer layer lightweight concrete on activated water with pH = 8.5).

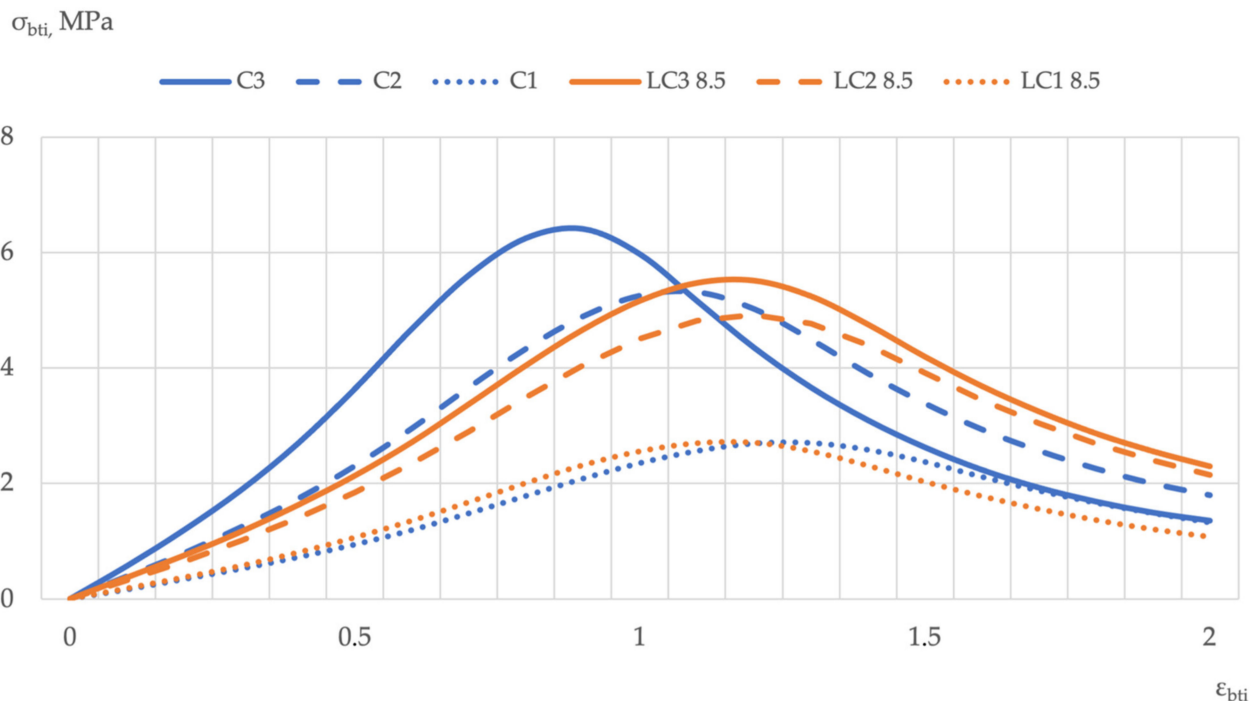


Figure 11. Diagram “stress—strain” in tension for the differential characteristics of vibro-centrifuged concrete (see Figure 10; C1, C2, C3—respectively the inner, middle, and outer layer of the control concrete composition; LC1 8.5, LC2 8.5, LC3 8.5—respectively the inner, middle, and outer layer lightweight concrete on activated water with pH = 8.5).

Based on the analysis results of the obtained strain diagrams, both of the entire sections were constructed according to the integral characteristics for vibro-centrifuged concrete. According to the differential characteristics built from the test results of samples

cut from layers of variatropic sections of vibro-centrifuged concrete, the following effects can be highlighted.

It was found that the use of water activated by alkalis affects the strain diagram of the resulting concrete as follows: the peak of the diagrams shifts up and to the right relative to the diagram of a control sample made of heavy concrete, which has a higher absolute strength, as well as the fragility of the nature of destruction.

Deformability, that is, both the ultimate compressibility and the ultimate tensility, increase, due to the more viscous and, accordingly, less brittle character of the prototype destruction. The absolute strength of the obtained samples is slightly reduced, but due to a significant decrease in density, the structural quality of the sample and its increased deformability contribute to the great possibilities of using such lightweight, more universal types of vibro-centrifuged concrete. Thus, according to the results of the analysis of the deformation diagrams, it is possible to conclude that the proposed method was effective.

4. Discussion

The studies carried out, reflected in the literature review, show that the main task of previous research was to improve the structure and mechanical and physical properties, for concrete of various densities, both heavy and lightweight due to the use of alkaline components. At the same time, only a few of them considered alkaline water, as most of them preferred to obtain an alkaline component through the use of a slag-alkaline binder. Furthermore, it was assumed that the use of slag and fly ash, in the correct dosage, with rational composition and technological parameters, would improve the characteristics and structure of concrete. The effect on the properties and structure of heavy and lightweight concrete has been noted. At the same time, there have been no previous studies aimed at investigating the effect of vibro-centrifuged factors on the characteristics and structure concrete, as well as any other centrifugally compacted concrete with the use of alkaline components: binders, water, or fillers [1–7,10–32].

It should be noted that only works [21,22] are devoted to the issue of structure and structure formation to a large extent, while in our study the issue of structure plays an important role. In addition, we are considering a more universal relative indicator-coefficients, in contrast to other works [1–7,10–32], where absolute indicators were considered.

Thus, the novelty and fundamental difference of the research carried out in this article is the control of the variatropy of concrete obtained by the centrifugal compaction method. Additionally, a feature is the effect on water, which allows the use of standard Portland cement, which is more traditional and, so far, the most widely used for these exclusive and special products and structures as centrifuged and vibro-centrifuged reinforced concrete elements.

At the same time, in our study, special attention is paid to the quantitative value of the pH index, which is very effective in certain ranges; however, if we go beyond this range, we can get a negative effect in the form of corrosive effects and other destructive consequences for the structure of concrete or its reinforcing elements. Additionally, one of the risks of the proposed technology is the possible occurrence of an alkali-silica reaction.

Thus, firstly, it is possible to note the novelty of the research carried out, its practical significance and applicability for reinforced concrete with an improved structure of concrete of annular section, and also determine the trajectory and vector of the direction of subsequent research.

In the future, the study of lightweight and heavy fiber concrete with variatropic and non-variatic structures on alkaline water, namely the interaction of water with rational alkaline indicators with metallic and non-metallic dispersed fibers, will be promising.

Additionally, a promising direction is a search for rational ways based on neural networks [40] of joint complex application of nanostructuring and nano-modifying components with water activated by alkalis in the composition of concrete to obtain the most effective types of products and structures.

Based on the comparison of our work with the research of other authors, we note that we have achieved the following scientific results for the first time.

From the point of view of fundamental science:

- received new knowledge about the processes of structure formation of variatropic concretes;
 - describes the physicochemical aspects of improving their performance characteristics with alkaline activation of water for concrete mixes.
- From the point of view of applied sciences:
- the practical dependences between the input technological factors and the output parameters of ready-mixed concrete are set and confirmed.

5. Conclusions

New knowledge has been obtained about the structure formation processes of variatropic concretes and the physicochemical aspects of improving their operational characteristics under alkaline activation of water for concrete mixtures. Based on the data obtained, a theory was formulated, and the applied relationships between the input technological factors and the output parameters of ready-mixed concrete were phenomenologically specified and confirmed.

The new proposed complex activation technology for vibro-centrifugation of concrete on water activated with alkali, subject to the recommendations developed by us on the rational values of recipe and technological factors, is effective and contributes to a change in the direction of improving the characteristics of concrete. An increase in physical and mechanical characteristics of up to 15–20% was obtained and the design and its performance were improved (the efficiency of improving the design, expressed as a percentage, reached values of more than 70% for control samples).

The theoretical substantiation and experimental confirmation of the results obtained are presented.

A positive effect on the properties of vibro-centrifuged concretes in general over the entire thickness of the annular section has been revealed. Thereby, a method for controlling the integral characteristics of concretes has been obtained.

The possibility of regulating the variatropic structure and controlling the differential characteristics of vibro-centrifuged concretes has been established.

An assessment of the constructive quality and variatropic efficiency of vibro-centrifuged concretes of a new type was carried out, new calculated dependencies were proposed, expressed in the form of relative coefficients.

The results obtained are recommended for implementation in practical production as an effective low-power-consuming method for obtaining improved building materials and structures from them.

Author Contributions: Conceptualization, L.R.M., S.A.S. and E.M.S.; methodology, L.R.M., A.N.B., S.A.S. and E.M.S.; software, S.A.S., E.M.S. and A.S.S.; validation, A.N.B., S.A.S. and E.M.S.; investigation, A.N.B., S.A.S., D.B. and E.M.S.; resources, B.M. and L.R.M.; data curation, A.N.B., S.A.S. and E.M.S.; writing—original draft preparation, A.N.B., S.A.S. and E.M.S.; writing—review and editing, A.N.B., S.A.S. and E.M.S.; visualization, D.B., A.S.S., S.A.S. and E.M.S.; supervision, B.M., A.N.B. and L.R.M.; project administration, L.R.M. and B.M.; funding acquisition, A.N.B., B.M. All authors have read and agreed to the published version of the manuscript.

Funding: This research was funded by Don State Technical University, Rostov-on-Don, Russia.

Institutional Review Board Statement: The study does not include human or animal research.

Informed Consent Statement: Not applicable.

Data Availability Statement: Data sharing not applicable.

Acknowledgments: The authors would like to acknowledge the administration of Don State Technical University for resource and financial support and personally to Besarion Meskhi.

Conflicts of Interest: The authors declare no conflict of interest. The funders had no role in the design of the study; in the collection, analyses, or interpretation of data; in the writing of the manuscript, or in the decision to publish the results.

References

1. Marvila, M.T.; de Azevedo, A.R.G.; de Matos, P.R.; Monteiro, S.N.; Vieira, C.M.F. Materials for Production of High and Ultra-High Performance Concrete: Review and Perspective of Possible Novel Materials. *Materials* **2021**, *14*, 4304. [[CrossRef](#)]
2. Anysz, H.; Narloch, P. Designing the composition of cement stabilized rammed earth using artificial neural networks. *Materials* **2019**, *12*, 1396. [[CrossRef](#)]
3. Gómez-Casero, M.A.; Pérez-Villarejo, L.; Castro, E.; Eliche-Quesada, D. Effect of steel slag and curing temperature on the improvement in technological properties of biomass bottom ash based alkali-activated materials. *Constr. Build. Mater.* **2021**, *302*, 124205. [[CrossRef](#)]
4. Sun, J.; Wang, Y.; Yao, X.; Ren, Z.; Zhang, G.; Zhang, C.; Chen, X.; Ma, W.; Wang, X. Machine-Learning-Aided Prediction of Flexural Strength and ASR Expansion for Waste Glass Cementitious Composite. *Appl. Sci.* **2021**, *11*, 6686. [[CrossRef](#)]
5. Al-Sodani, K.A.A.; Adewumi, A.A.; Mohd Ariffin, M.A.; Maslehuddin, M.; Ismail, M.; Salami, H.O.; Owolabi, T.O.; Mohamed, H.D. Experimental and Modelling of Alkali-Activated Mortar Compressive Strength Using Hybrid Support Vector Regression and Genetic Algorithm. *Materials* **2021**, *14*, 3049. [[CrossRef](#)] [[PubMed](#)]
6. Amran, M.; Fediuk, R.; Murali, G.; Avudaiappan, S.; Ozbakkaloglu, T.; Vatin, N.; Karelina, M.; Klyuev, S.; Gholampour, A. Fly Ash-Based Eco-Efficient Concretes: A Comprehensive Review of the Short-Term Properties. *Materials* **2021**, *14*, 4264. [[CrossRef](#)] [[PubMed](#)]
7. Balun, B.; Karataş, M. Influence of curing conditions on pumice-based alkali-activated composites incorporating Portland cement. *J. Build. Eng.* **2021**, *43*, 102605. [[CrossRef](#)]
8. Mailyan, L.R.; Stel'makh, S.A.; Shcherban', E.M.; Khalyushev, A.K.; Smolyanichenko, A.S.; Sysoev, A.K.; Parinov, I.A.; Cherpakov, A.V. Investigation of Integral and Differential Characteristics of Variatropic Structure Heavy Concretes by Ultrasonic Methods. *Appl. Sci.* **2021**, *11*, 3591. [[CrossRef](#)]
9. Stel'makh, S.A.; Shcherban', E.M.; Shuiskii, A.I.; Prokopov, A.Y.; Madatyan, S.M.; Parinov, I.A.; Cherpakov, A.V. Effects of the Geometric Parameters of Mixer on the Mixing Process of Foam Concrete Mixture and Its Energy Efficiency. *Appl. Sci.* **2020**, *10*, 8055. [[CrossRef](#)]
10. Tekle, B.H.; Holschemacher, K.; Löber, P.; Heiden, B. Mechanical Behavior and Frost-Resistance of Alkali-Activated Cement Concrete with Blended Binder at Ambient Curing Condition. *Buildings* **2021**, *11*, 52. [[CrossRef](#)]
11. Marvila, M.T.; Azevedo, A.R.G.; Vieira, C.M.F. Reaction mechanisms of alkali-activated materials. *Rev. IBRACON Estrut. Mater.* **2021**, *14*, e14309. [[CrossRef](#)]
12. Ding, Y.; Dai, J.G.; Shi, C.J. Mechanical properties of alkali-activated concrete: A state-of-the-art review. *Constr. Build. Mater.* **2016**, *127*, 68–79. [[CrossRef](#)]
13. Khan, M.; Saha, A.K.; Sarker, P.K. Evaluation of the ASR of waste glass fine aggregate in alkali activated concrete by concrete prism tests. *Constr. Build. Mater.* **2021**, *266*, 121121. [[CrossRef](#)]
14. Siddique, S.; Kim, H.; Son, H.; Jang, J.G. Characteristics of Preplaced Aggregate Concrete Fabricated with Alkali-Activated Slag/Fly Ash Cements. *Materials* **2021**, *14*, 591. [[CrossRef](#)]
15. Altan, E.; Erdoğan, S.T. Alkali activation of a slag at ambient and elevated temperatures. *Cem. Concr. Comp.* **2012**, *34*, 131–139. [[CrossRef](#)]
16. Shi, C.; Hu, X.; Zhao, R.; Chong, L.; Shi, Z. A review on alkali-aggregate reactions in alkali-activated mortars/concretes made with alkali-reactive aggregates. *Mater. Struct.* **2015**, *48*, 621–628. [[CrossRef](#)]
17. Krivenko, P.; Gelevera, O.; Kovalchuk, O.; Bumanis, G.; Korjakins, A. Alkali-aggregate reaction in alkali-activated cement concretes. *IOP Conf. Ser. Mater. Sci. Eng.* **2019**, *660*, 012002. [[CrossRef](#)]
18. Wang, H.; Wu, Y.; Wang, L.; Chen, H.; Cheng, B. Properties of a Lightweight Fly Ash-Slag Alkali-Activated Concrete with Three Strength Grades. *Appl. Sci.* **2021**, *11*, 766. [[CrossRef](#)]
19. Yliniemi, J.; Nugteren, H.; Illikainen, M.; Tiainen, M.; Weststrate, R.; Niinimäki, J. Lightweight aggregates produced by granulation of peat-wood fly ash with alkali activator. *Int. J. Miner. Process.* **2016**, *149*, 42–49. [[CrossRef](#)]
20. Bilek, V.; Sucharda, O.; Bujdos, D. Frost Resistance of Alkali-Activated Concrete—An Important Pillar of Their Sustainability. *Sustainability* **2021**, *13*, 473. [[CrossRef](#)]
21. Provis, J.L. Alkali-activated materials. *Cem. Concr. Res.* **2018**, *114*, 40–48. [[CrossRef](#)]
22. Luukkonen, T.; Abdollahnejad, Z.; Yliniemi, J.; Kinnunen, P.; Illikainen, M. One-part alkali-activated materials: A review. *Cem. Concr. Res.* **2018**, *103*, 21–34. [[CrossRef](#)]
23. Shagñay, S.; Velasco, F.; Torres-Carrasco, M.; Del Campo, A. Wear behavior in pastes of alkali-activated materials: Influence of precursor and alkali solution. *Tribol. Int.* **2020**, *147*, 1–10. [[CrossRef](#)]
24. Zhu, H.; Yang, S.; Li, W.; Li, Z.; Fan, J.; Shen, Z. Study of Mechanical Properties and Durability of Alkali-Activated Coal Gangue-Slag Concrete. *Materials* **2020**, *13*, 5576. [[CrossRef](#)] [[PubMed](#)]
25. Provis, J.L.; Bernal, S.A. Geopolymers and Related Alkali-Activated Material. *Annu. Rev. Mater. Res.* **2014**, *44*, 299–327. [[CrossRef](#)]

26. Villaquirán-Cacedo, M.A.; Mejíade Gutiérrez, R. Synthesis of ceramic materials from ecofriendly geopolymer precursors. *Mater. Lett.* **2018**, *1*, 300–304. [[CrossRef](#)]
27. Cai, J.; Pan, J.; Li, X.; Tan, J.; Li, J. Electrical resistivity of fly ash and metakaolin based geopolymers. *Constr. Build. Mater.* **2020**, *234*, 117868. [[CrossRef](#)]
28. Wei, X.; Ming, F.; Li, D.; Chen, L.; Liu, Y. Influence of Water Content on Mechanical Strength and Microstructure of Alkali-Activated Fly Ash/GGBFS Mortars Cured at Cold and Polar Regions. *Materials* **2020**, *13*, 138. [[CrossRef](#)]
29. El-Hassan, H.; Hussein, A.; Medlji, J.; El-Maaddawy, T. Performance of Steel Fiber-Reinforced Alkali-Activated Slag-Fly Ash Blended Concrete Incorporating Recycled Concrete Aggregates and Dune Sand. *Buildings* **2021**, *11*, 327. [[CrossRef](#)]
30. Risdanareni, P.; Van den Heede, P.; Wang, J.; De Belie, N. The Durability of Mortar Containing Alkali Activated Fly Ash-Based Lightweight Aggregate. *Materials* **2021**, *14*, 3741. [[CrossRef](#)]
31. Tekle, B.H.; Hertwig, L.; Holschemacher, K. Setting Time and Strength Monitoring of Alkali-Activated Cement Mixtures by Ultrasonic Testing. *Materials* **2021**, *14*, 1889. [[CrossRef](#)]
32. Serpokyrov, N.S.; Smolyanichenko, A.S.; Starovoitov, S.V. Features of the water treatment technology of fish breeding plants in the southern region of the Russian Federation using agricultural waste. *E3S Web Conf.* **2021**, *175*, 02009. [[CrossRef](#)]
33. Stel'makh, S.A.; Shcherban', E.M.; Kholodnyak, M.G.; Nasevich, A.S.; Yanovskaya, A.V. Pat. 197610 Russian Federation, MPK B28B 21/30Rostov-on-Don. DSTU. N 2020103753; declared 29.01.20; publ. 18.05.20, bull. N 14. 4p. Available online: <https://patentimages.storage.googleapis.com/99/a7/e4/7331df00d4bdba/RU197610U1.pdf> (accessed on 4 October 2021).
34. Mailyan, L.R.; Beskopylny, A.N.; Meskhi, B.; Stel'makh, S.A.; Shcherban, E.M.; Ananova, O. Optimization of Composition and Technological Factors for the Lightweight Fiber-Reinforced Concrete Production on a Combined Aggregate with an Increased Coefficient of Structural Quality. *Appl. Sci.* **2021**, *11*, 7284. [[CrossRef](#)]
35. Mailyan, L.R.; Beskopylny, A.N.; Meskhi, B.; Shilov, A.V.; Stel'makh, S.A.; Shcherban', E.M.; Smolyanichenko, A.S.; El'shaeva, D. Improving the Structural Characteristics of Heavy Concrete by Combined Disperse Reinforcement. *Appl. Sci.* **2021**, *11*, 6031. [[CrossRef](#)]
36. GOST 10180 Concretes. Methods for Strength Determination Using Reference Specimens. Available online: <http://docs.cntd.ru/document/1200100908> (accessed on 4 October 2021).
37. GOST 24452 Concretes. Methods of Prismatic, Compressive Strength, Modulus of Elasticity and Poisson's Ratio Determination. Available online: <https://docs.cntd.ru/document/9056198> (accessed on 4 October 2021).
38. GOST 10181 Concrete Mixtures. Methods of Testing. Available online: <https://docs.cntd.ru/document/1200115733> (accessed on 4 October 2021).
39. GOST 23732-2011 Water for Concrete and Mortars. Specifications. Available online: <https://docs.cntd.ru/document/1200093835> (accessed on 4 October 2021).
40. Beskopylny, A.; Lyapin, A.; Anysz, H.; Meskhi, B.; Veremeenko, A.; Mozgovoy, A. Artificial neural networks in classification of steel grades based on non-destructive tests. *Materials* **2020**, *13*, 2445. [[CrossRef](#)] [[PubMed](#)]